Carbohydrate Polymers 96 (2013) 376–383

Contents lists available at SciVerse ScienceDirect

Carbohydrate Polymers

journal homepage: www.elsevier.com/locate/carbpol

Antitumor activity of *Portulaca oleracea* L. polysaccharides against cervical carcinoma in vitro and in vivo

Rui Zhao[a,b], Xu Gao[b,*], Yaping Cai[a], Xingyue Shao[c], Guiyan Jia[a], Yulan Huang[a], Xuegong Qin[a], Jingwei Wang[a], Xiaoliang Zheng[a]

[a] *Department of Pharmaceutical Engineering, College of Life Science & Biotechnology, Heilongjiang August First Land Reclamation University, Daqing High-Tech Industrial Development Zone, 163319 PR China*
[b] *Department of Biochemistry and Molecular Biology, Basic Medical Science College, Harbin Medical University, Harbin 150081, PR China*
[c] *Department of Gynaecology and Obstetrics, Daqing Oilfield Hospital, Daqing 163311, PR China*

ARTICLE INFO

Article history:
Received 17 October 2012
Received in revised form 18 March 2013
Accepted 10 April 2013
Available online 17 April 2013

Keywords:
Polysaccharides
Portulaca oleracea L.
Cervical carcinoma
Cell cycle
Apoptosis

ABSTRACT

Portulaca oleracea L. has been used as folk medicine in different countries to treat different ailments in humans. *P. oleracea* L. polysaccharide (POL-P), extracted from *P. oleracea* L., is found to have bioactivities such as hypoglycemic and hypolipidemic activities, antioxidant and antitumor activities. In our study, a water-soluble polysaccharide (POL-P3b) was successfully purified from *Galium verum* L. by DEAE cellulose and Sephadex G-200 column chromatography. To evaluate the anticancer efficacy and associated mechanisms of POL-P3b on cervical cancer in vitro and in vivo, we showed that treatment of HeLa cell with POL-P3b inhibited cell proliferation. In addition, POL-P3b significantly inhibited tumor growth in U14-bearing mice. Further analysis indicated that POL-P3b possesses the activity of inhibiting cervical cancer cell growth in vitro and in vivo at a concentration- and time-dependent manner, and the mechanisms were associated with Sub-G1 phase cell cycle arrest, triggering DNA damage and inducing apoptosis.

1. Introduction

Cervical carcinoma is the second most prevalent cancer affecting women worldwide, and 500,000 new cases are reported per year. The incidence is higher in Asia, South America, and Africa (Peter & Krammer, 2003). Chemotherapy is the most common treatment for cancer. Unfortunately, many of the chemotherapeutic drugs are non-specific and cause severe side effects. Therefore, searching for new alternative strategies for the prevention and treatment of cervical cancer is essential. Natural products, including plants, microorganisms and marines, have been considered as a valuable source for anticancer drug discovery (Schwartsmann et al., 2002). *Portulaca oleracea* L. has been used as folk medicine in different countries to treat different ailments in humans. It is known as a "vegetable for long life" in Chinese folklore and is sold in shops in the United Arab Emirates and Oman (Xiang et al., 2005). People in Jordan use *P. oleracea* L. as food either raw in salad or cooked as a vegetable dish. *P. oleracea* L. polysaccharide (POL-P), extracted from *P. oleracea* L., is found to have bioactivities such as hypoglycemic and hypolipidemic activities, antioxidant and antitumor activities (Chen et al., 2011). However, very little is known about the identification of compounds from POL-P and the anticancer effects on cervical cancer. Nearly 100 botanical polysaccharides are considered as important bioactive components responsible for antitumor effect, such as polysaccharide isolated from Zizyphus jujuba and Solanum nigrum (Hung, Hsu, Chang, & Chen, 2012).

There are two pathways by which death signals are transduced to the cellular apoptotic mechanism: an extrinsic pathway via a cell surface receptor and an intrinsic pathway through mitochondria. The mitochondria-mediated apoptotic pathway is activated by a death signal, which leads to the activation of Bax involving release of cytochrome *c* from the mitochondrial intermembrane space into the cytosol. The released cytochrome *c* by binding to Apaf-1 activates procaspase-9, and the latter in turn activates caspase-3 and other effector caspases. It has been reported that p53 can act as a trans-activator or repressor for a set of pro- or antiapoptotic genes. DNA damage is a common event in life following which; repair mechanisms and apoptosis will be activated to maintain genome integrity. The tumor-suppressor protein p53 provides an important link between DNA damage and apoptosis. DNA damage results in cell cycle arrest at checkpoints or at G1 or G2 stage to inhibit cell cycle progression and to induce apoptosis.

In the present study, we investigated the anticancer effects and associated mechanisms of POL-P3b, the major constituent of POL-P on cervical cancer in vitro and in vivo.

* Corresponding author at: Department of Biochemistry and Molecular Biology, Basic Medical Science College, Harbin Medical University, 194 XueFu Road, Nangang Dist, Harbin 150081, PR China. Tel.: +86 451 87086131; fax: +86 451 87086131.
E-mail address: zhaoruier@sina.com (X. Gao).

0144-8617/$ – see front matter © 2013 Elsevier Ltd. All rights reserved.
http://dx.doi.org/10.1016/j.carbpol.2013.04.023

2. Materials and methods

2.1. Materials

MTT [3-(4,5-dimethylthiazol-2-yl)-2,5-diphenyl-2*H*-tetrazolium bromide] and Hoechst 33342 were from Sigma. The terminal deoxynucleotidyl transferase (TdT)-catalyzed dUTP-nick end labeling (TUNEL) In Situ Cell Death Detection Kit was the product of Roche Molecular Biochemicals (Basel, Switzerland). Antibodies against cytochrome *c*, P53 and caspase 3, 8, 9 were purchased from Santa Cruz Biotechnology, Inc. (Santa Cruz, CA). All other reagents and chemicals were of the highest purity grade available.

2.2. Preparation of POL-P3b from Portulaca oleracea L.

P. oleracea L. was collected in October 2011 from Heilongjiang province, China. The whole plant was dried in the shade and authenticated by Dr. X.Z. Han at Heilongjiang University of Chinese medicine, China, where the herbarium voucher has been kept. The method used for preparation of crude polysaccharides from *P. oleracea* L. is based on the previous method (Li et al., 2010). Briefly, dry *P. oleracea* L. (500 g) was refluxed with methanol to remove lipids, and then refluxed with 80% ethanol twice to remove oligosaccharides. The residue soaked in 2000 ml distilled water and boiled at 95 °C for 6 h, subsequently filtered. The collected crude extract was mixed with 50 mL of 95% ethanol in a centrifuge tube, after which the solution was left standing at 4 °C for 24 h for precipitation and then centrifuged at 9000 rpm for 30 min. The supernatant was removed and the precipitate was freeze dried to obtain a crude polysaccharide powder. Next, 0.8 g of crude polysaccharide was collected and mixed with 100 mL of PBS (pH 8), followed by shaking in a 50 °C water bath for 2 h, the addition of 5 mL papain, and shaking in a 70 °C water bath for 4 h for protein digestion. The concentrated solution was centrifuged at 9000 rpm for 15 min and the supernatant was collected, followed by pouring into a dialysis bag (45 cm × 50 cm, Germany). Crude polysaccharide was eluted and isolated on DEAE cellulose column (ø25 mm × 350 mm) with distilled water and 0.05–0.5 mol/L NaCl. The collected three fractions were dialyzed, centrifuged, and freeze-dried. For gel permeation chromatography, samples were dissolved in 20 ml of buffer, then applied to a Sephadex G-200 column (ø20 mm × 750 mm), and eluted with 0.05 mol/L NaCl at a flow rate of 0.5 ml/min. The fractions were collected using an elution pattern and concentrated in an evaporator at 60 °C. The concentrate was dialyzed in distilled water for 72 h, and then freeze-dried. The amount of polysaccharide was quantified using a phenol–sulfuric acid method (Chang, Hsu, & Chen, 2010). The structure of polysaccharide fraction was detected by ultraviolet (UV) and infrared spectroscopy (IR).

2.3. Determination of molecular weight (MW) and monosaccharide composition of POL-P3b

The high performance liquid chromatography (HPLC) system was used to determine the MW of POL-P3b. The MW was determined by comparison with retention time of pullulan standard. One-hundred μl of POL-P3b, with the concentration 4–5 g/L, were hydrolyzed with 100 μl 4 mol/L TFA at 110 °C for 2 h. After removing TFA with methanol, samples were dissolved in NaOH and pre-column derivated with 1-phenyl-3-methyl-5-pyrazolone (PMP) using the method described by Zhao, Dong, Chen, and Hu (2010). The PMP derivatives of the standard sugars (Mannose, Ribose, Rhamnose, Glucuronic acid, Glucose, Galactose, Xylose) and POL-P3b were subjected to HPLC (Dionex Co., America), fitted with EclipseXPB-C18 Column (4.6 mm × 250 mm).

2.4. Cell lines and culture

The human cervical cancer HeLa and the mouse cervical carcinoma U14 cells were obtained from the Cell Bank of Institute of Basic Medical Sciences (Peking Union Medical College, Beijing, China). Cells were cultured in Dulbecco's modified Eagle's medium (DMEM; high glucose, Gibco) supplemented with 10% fetal bovine serum (FBS, Hyclone).

2.5. MTT cell proliferation assay

The growth inhibitory effect of POL-P3b on HeLa cells was determined by measuring MTT dye absorbance in living cells. Briefly, cells were seeded in 96-well plates at density of 5000–10,000 cells/well. After treatment with different concentrations of POL-P3b for 24, 48 and 72 h, MTT was added to each well at a final concentration of 0.4 mg/ml and further incubated for 3 h at 37 °C. The MTT solution in medium was then removed. To solubilize formazan crystals formed in viable cells, 100 μl dimethyl sulfoxide (DMSO) was added to each well before the absorbance at 540 nm was measured using a microplate ELISA reader (Model 550, Bio-Rad, USA). Results were expressed as the percentage of 100% (control) proliferation. The IC50 value was expressed as the concentration of POL-P3b that inhibited the growth of cells by 50%.

2.6. Hoechst 33342 staining

Cells seeded in chamber slides were treated with POL-P3b (250, 500 and 1000 μg/mL). At the indicated times the medium was removed, and the cells were washed twice with PBS, fixed in 3% paraformaldehyde for 20 min, then rewashed, and stained with Hoechst 33342 (10 μg/ml) at 37 °C for 20 min in the dark. After washing with PBS for three times, the slides were covered with coverslips and observed in blue channel fluorescence immediately with fluorescent microscopy (OLYMPUS, CKX41-F32FL, Japan).

2.7. Cell cycle analysis

Cell cycle analysis was carried out by FACScan flow cytometer using standard protocol. The distribution of cells in the different cell-cycle phases was analyzed using Multicycle software (Phoenix Flow Systems, San Diego, CA). The percentage of cells in each phase of the cell cycle was determined at least triplicate and expressed as mean ± SD.

2.8. Detection of DNA damage by the comet assay

Cells were treated with POL-P3b for 48 h in complete medium, and the comet assay procedure in this study was a modification of the method described earlier (Wu, Guo, & Zhao, 2006). For each sample, the tail lengths of a minimum of 50 comets were analyzed. Mean comet tail moments based on 100 comet image analysis per slide after treatment with various concentrations of POL-P3b. The length of the comet was quantified as the distance from the centrum of the cell nucleus to the tip of the tail in pixel units. The tail moment, expressed in arbitrary units, has been calculated by multiplying the percent of DNA (fluorescence) in the tail by the length of the tail.

2.9. Analysis of cytochrome c expression and measurement of caspase-3, 8, 9 and P53 activities

After treatment with the given concentrations of POL-P3b for 72 h, cells were collected. The protein in the cytosolic fraction and total protein were measured by the Bradford assay using bovine serum albumin as the standard and cytochrome *c*, caspase-3, 8, 9

and P53 were detected by Western blot analysis. The bands of the proteins were visualized using the ECL Dura^{TM} chemiluminescence detection system.

2.10. Animal experiment design

Female Kunming mice (6–8 w, 18–22 g) were provided by the Experimental Animal Center of Hayida Medical University. The animals were treated according to the National Institute of Health Guide for the Care and Use of Laboratory Animals and further approval for their experimentation was obtained from the Animal Ethics Committee of the university.

The U14 mouse cervical carcinoma cells were used in animal experiments to study the in vivo antitumor efficacy of POL-P3b. For analysis of therapeutic efficacy in the intraperitoneal model, U14 cells (1×10^7 cells in 1 mL of sterile physiological saline) were ip injected. After 24 h, mice were randomly divided into four groups (10 mice per group) and gavaged with sterile water (control group) or various doses of POL-P3b (L: 50 mg/kg, M: 100 mg/kg, H: 200 mg/kg) in sterile water (treatment groups) once a day. All groups were continuously treated for 12 days. On day 13 of the experiment, all animals were sacrificed, and the transplanted tumors of treated and control mice were harvested and weighed. The tumor inhibition rate was expressed according to the following formula: (the mean tumor weight of control group − the mean tumor weight of treated group)/the mean tumor weight of control group × 100. Half of the tumor tissue was fixed in 4% paraformaldehyde in PBS and embedded in paraffin for TUNEL analysis.

2.11. Apoptosis detection of tumor tissue by TUNEL staining

All tumor sections (5 μm) were de-waxed and processed conventionally. TUNEL tests of paraffin slides were performed using a commercial kit, following the manufacturer's instructions. The slides were counterstained with hematoxylin and viewed under a light microscope.

2.12. Statistical analysis

All the grouped data were statistically evaluated with SPSS/13.0 software. Statistical analysis was performed by one-way analysis of variance (ANOVA). *P*-values of less than 0.05 were considered to be significant. All the results were expressed as the mean ± S.D.

3. Results

3.1. Isolation, purification and characterization of POL-P3b

POL-P was obtained by water extraction and ethanol precipitation, and then subjected to DEAE-cellulose ion exchange chromatography with NaCl elution resulting in POL-P1, POL-P2 and POL-P3 peaks (Fig. 1A). According to the sugar content of various subfraction and growth inhibitory effect on HeLa cells in preliminary experiment, we screened that POL-P3 was the most effective, therefore, the further separation and purification for POL-P3. The POL-P3 fraction (100 mg) was further separated into POL-P3a and POL-P3b by Sephadex G-200 gel chromatography column (Fig. 1B). POL-P3b was identified to be homogeneous polysaccharide component, which showed a single symmetrical peak through gel filtration chromatography (Fig. 1C). The MW distribution of POL-P3b was 253,688 Da and retention times of 8.146 min (Fig. 1D). The MW distribution in POL-P3b was determined based on the standard curve of pullulan. The linear regression equation of $y = -0.415x + 8.7849$ with a correlation coefficient (R^2) of 0.9942 was obtained. POL-P3b had one absorption peaks at 200 nm and had no absorption at 260 and 280 nm in the UV spectrum (Fig. 1E), indicating the absence of protein and nucleic acid. As shown in Fig. 1F, according to IR spectra, the purified POL-P3b displayed a broadly stretched intense peak at 3445 cm^{-1} characteristic of hydroxyl groups and a weak C—H peak at around 2921 cm^{-1}. The relatively strong absorption peak at around 1640 cm^{-1} indicated the absorbed water. The absorbance of polysaccharides in 1085 cm^{-1} was the C—O—H link band positions. The absorption peak at 895 cm^{-1} indicated the existence of β-glycosidic linkage. Analysis of sugar composition of POL-P3b indicated that both polysaccharides consisted primarily of glucose and galactose, and the molar ration was 0.75:1.00.

Table 1
Effects of POL-P3b on proliferation of HeLa cells ($\bar{x} \pm$ S.D.).

POL-P3b (μg/mL)	Inhibition rate (%)		
	24 h	48 h	72 h
0	–	–	–
50	3.1 ± 0.1	6.5 ± 0.2	9.2 ± 0.4
100	8.9 ± 0.2	17.7 ± 0.3	29.9 ± 0.6
250	20.3 ± 0.4	30.9 ± 1.2	43.5 ± 1.6
500	31.2 ± 1.8	51.8 ± 2.1	63.6 ± 2.7
1000	43.8 ± 2.3	68.7 ± 2.8	88.9 ± 3.2

3.2. Inhibition of HeLa cell proliferation by POL-P3b in a dose- and time-dependent manner

As shown in Table 1, POL-P3b inhibited cell proliferation at dose- and time-dependent manners. POL-P3b from 100 to 1000 μg/mL had exerted potent inhibitory effects on HeLa cell growth. By 48 h after POL-P3b 500 μg/mL treatment, the cell death rate reached almost 50%. The IC50 values at 24, 48 and 72 h were 1225.32, 489.17 and 407.23 (μg/mL), respectively. Therefore, 48 h incubation with POL-P3b seemed to be sufficient for the half induction of cell death.

3.3. Effects of POL-P3b on tumor growth and weight of U14-bearing mice

The tumor weight of the POL-P3b (M), and POL-P3b (H) treatment groups was significantly lower than that of the control group ($P < 0.05$, $P < 0.01$, respectively). The tumor inhibition rate in the POL-P3b (L), POL-P3b (M), and POL-P3b (H) groups was 5.81, 24.59%, and 50.28%, respectively (Table 2). Moreover, the weight of U14-bearing mice in POL-P3b (H) treatment group was significantly increased.

3.4. POL-P3b induced apoptosis in U14-bearing mice

To consider the possibility that POL-P3b induced apoptosis in vivo, paraffin-embedded sections of tumors were analyzed by TUNEL assay. In the control group, the structure of cells was intact and the nucleus was completely stained blue (Fig. 2a). However, in the POL-P3b-treated group, the percentage of TUNEL-positive cells (brown) markedly increased (Fig. 2b–d), suggesting the increase in apoptotic tumor cells after POL-P3b treatment.

3.5. Effect of POL-P3b on Hoechst 33342 staining and the cell cycle distribution

The morphology of POL-P3b-treated HeLa cells exhibited typical apoptotic features, such as, cell shrinkage, rounding up, and detachment from the culture plate (Fig. 3A), in addition to nuclear breakdown and chromatin condensation (shown by arrows in Fig. 3A b–d), which were determined by staining nuclei with Hoechst 33342.

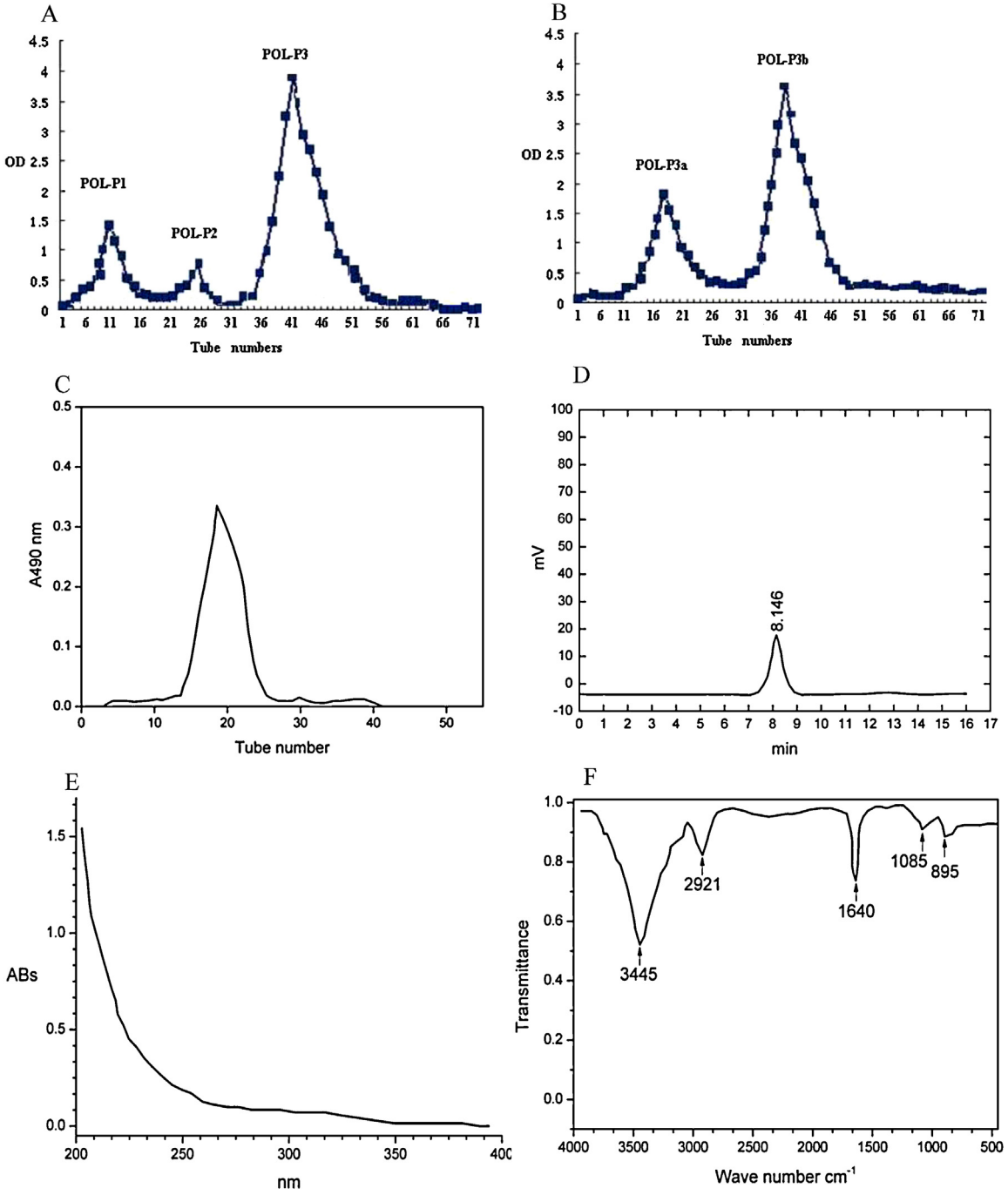

Fig. 1. Isolation, purification and characterization of POL-P3b. Fractionation of *Portulaca oleracea* L. polysaccharides by size-exclusion chromatography. (Panel A) Polysaccharides from crude *Portulaca oleracea* L. extract were isolated by DEAE-cellulose chromatography. The eluate of POL-P3 was further fractionated using Sephadex G-200 column chromatography (Panel B). Purity identification of POL-P1 by gel filtration chromatography (Panel C). High-performance gel filtration chromatograms of MW distribution of deproteinized POL-P3b (Panel D). The UV spectra of POL-P3b (Panel E). The IR spectra of POL-P3b (Panel F). (For interpretation of the references to spectra in figure legend, the reader is referred to the web version of the article.)

Table 2
Effects of POL-P3b on tumor growth and weight of U14-bearing mice ($\bar{x} \pm$ S.D.).

Groups	Animal number		Body weight (g)		Tumor weight (g)	Inhibition rate (%)
	Beginning	End	Beginning	End		
Control	10	8	21.35 ± 1.73	23.07 ± 1.81	3.62 ± 0.35	
POL-P3b (L)	10	10	20.88 ± 1.84	20.54 ± 1.72	3.41 ± 0.28	5.81
POL-P3b (M)	10	10	21.96 ± 1.87	24.71 ± 2.03	2.73 ± 0.60*	24.59
POL-P3b (H)	10	10	21.49 ± 1.71	25.62 ± 2.11*	1.80 ± 1.02**	50.28

Compared with control.
* $P < 0.05$.
** $P < 0.01$.

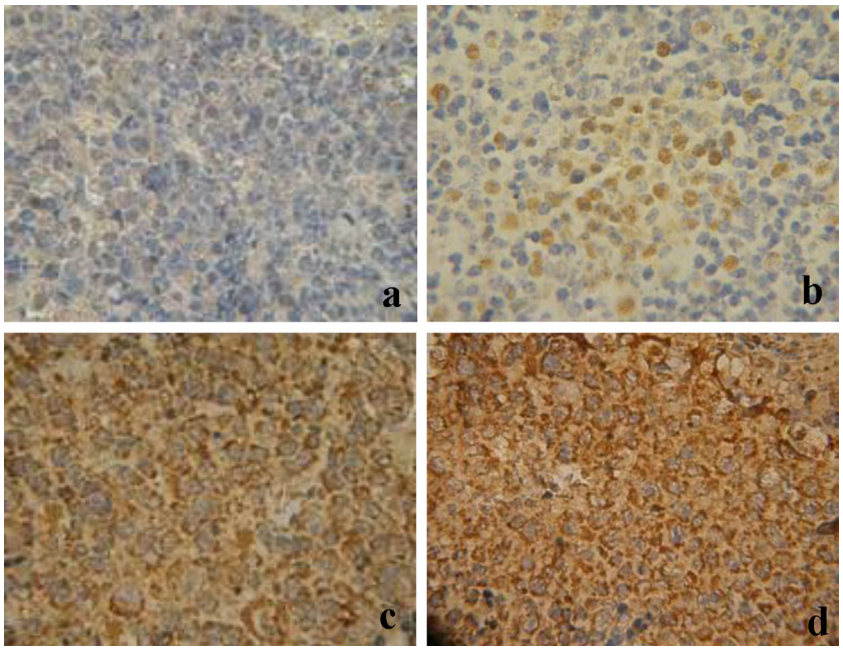

Fig. 2. Apoptosis analysis of tumor tissues by TUNEL staining. (a) In the control group, the nuclei of tumor cells were completely stained blue. (b)–(d) In the POL-P3b -treated group, apoptotic cells were scattered throughout the tissue section and intensely stained brown. (For interpretation of the references to color in figure legend, the reader is referred to the web version of the article.)

To determine if POL-P3b regulates cell cycle, HeLa cells were treated with POL-P3b for 72 h, and the distribution of cells in various compartments of the cell cycle was analyzed by flow cytometry. The induction of apoptosis was confirmed by the presence of the Sub-G1 cell population in flow cytometric analysis. The percentage of cells in each phase of cell cycle in control and treated groups were summarized in Fig. 3B. Compared with control, an accumulation of HeLa cells in the Sub-G1 phase (8.62–45.32%) was noticed in various POL-P3b concentrations.

3.6. Effect of POL-P3b on DNA damage

As shown in Fig. 4 and Table 3, treatment of HeLa cells with various concentrations of POL-P3b for 48 h resulted in a significant increase in percent of cells with tails, tail length and tail moment at dose-dependent manners. DNA damaging effect in terms of DNA fragmentation was determined by measuring the tail length and tail moment of the comet under microscope and casp software.

3.7. POL-P3b treatment regulated the intrinsic apoptotic pathway

We investigated the involvement of the mitochondrial-mediated intrinsic apoptotic pathway by assessing the release of cytochrome *c* from the mitochondria into the cytoplasm, and the cleavage of the caspase cascade. As shown in Fig. 5C, a significant increase in cytochrome *c* release was observed when HeLa cells were treated with POL-P3b, and this release was found to be dose-dependent. We also assessed the expression of tumor suppressor protein p53, and the result showed that POL-P3b mediated apoptosis in a p53-dependent manner (Fig. 5B). In addition, caspases have been reported to play vital roles in executing apoptosis. To identify the role of caspase involved in the signaling of apoptosis induced by POL-P3b, caspase-3, -8 and caspase-9 activities were assayed. The treatment of HeLa cells with various concentrations of POL-P3b for 72 h, significant increases of both caspase-9 and -3 activities were detected and found to be in a dose-dependent manner compared with the control (Fig. 5A), but caspase-8 activity did not change at various concentrations (Fig. 5A). The results suggested that POL-P3b-induced apoptosis occurred through the activation of the intrinsic mitochondrial apoptotic pathway in HeLa cells.

Table 3
Effect of POL-P3b on DNA damage ($\bar{x} \pm$ S.D.).

Groups	Percent of cells with tails (%)	Tail length (μm)	Tail moment
Control	6.12 ± 1.02	7.34 ± 1.08	1.56 ± 0.47
POL-P3b (L)	32.19 ± 1.43*	20.21 ± 1.27*	3.82 ± 1.51*
POL-P3b (M)	53.43 ± 2.66**	51.75 ± 2.82**	12.74 ± 0.78**
POL-P3b (H)	75.61 ± 3.78**	65.47 ± 3.27**	18.86 ± 0.97**

Compared with control.
* $P < 0.05$.
** $P < 0.01$.

4. Discussion

In the present study, *P. oleracea* L. polysaccharide (POL-P) was obtained through a series procedure of hot water extraction, ethanol precipitation, dialysis and lyophilization. For the first time, we obtained a water-soluble homogeneous polysaccharide POL-P3b by DEAE cellulose and Sephadex G-200 column chromatography and confirmed its anticancer activity. POL-P3b possessed relative higher antitumor activity in vitro than other *P. oleracea* L. polysaccharide. The differences in antitumor activity among the various polysaccharide fractions were probably due to their different monosaccharide composition, since it has been reported that the antitumor activity of polysaccharide might depend on its monosaccharide composition, molecular weight and structure of the polymeric backbone (Cui et al., 2007; Tao, Zhang, & Zhang, 2009). The relatively higher molecular mass and better water solubility seemed to increase the antitumor activities. Our results showed the molecular weight distribution of POL-P3b was 253,688 Da and the structure of the backbone displayed in Fig. 1F. Analysis of sugar composition of POL-P3b indicated that both polysaccharides consisted primarily of glucose and galactose, and the molar ration was 0.75:1.00.

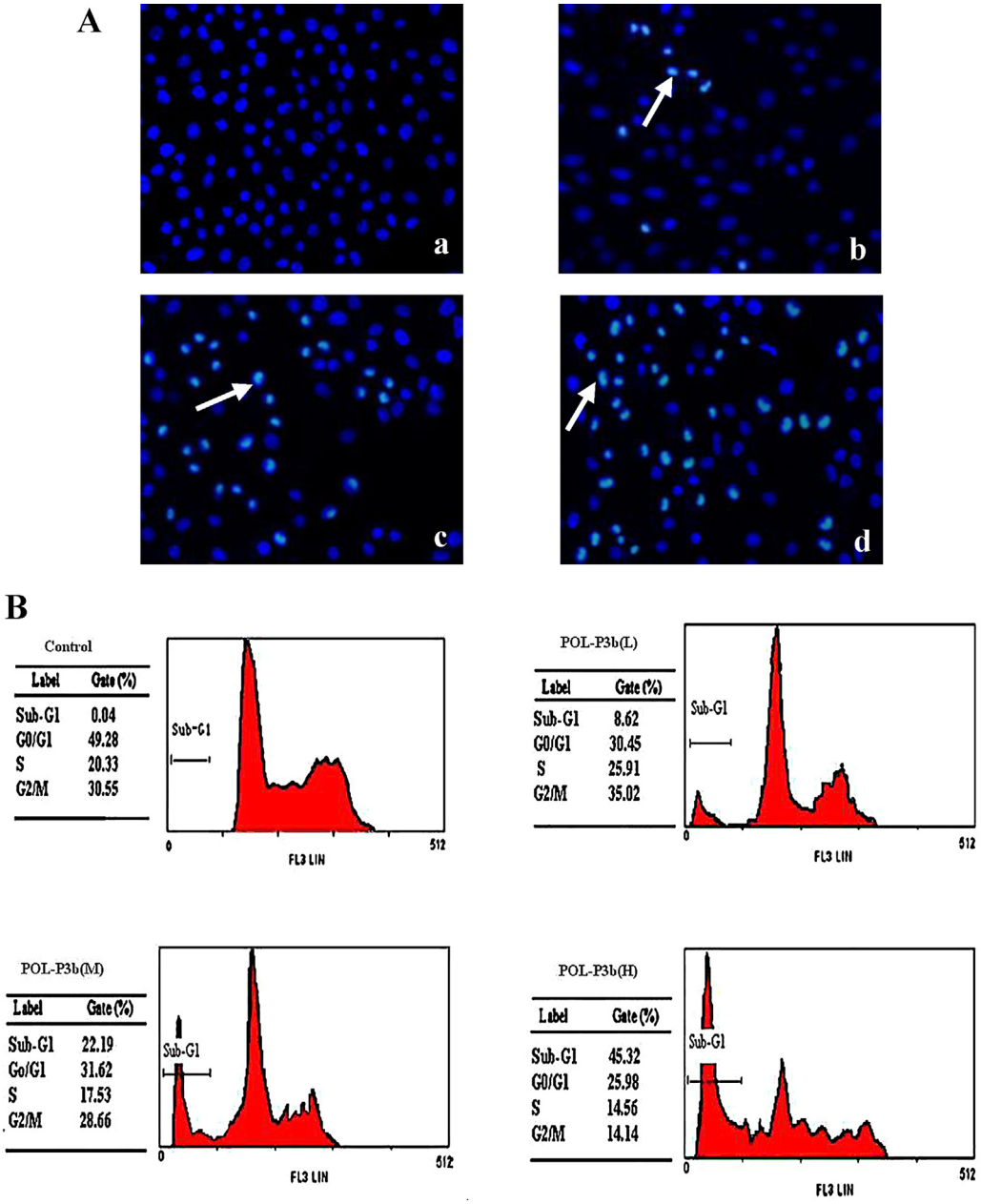

Fig. 3. Effect of POL-P3b on Hoechst 33342 staining and cell cycle distribution in cultured HeLa cells. (A) The morphologic changes of HeLa cells treated with POL-P3b for 72 h observed by fluorescence microscopy after nuclei staining with Hoechst 33342. (B) Flow cytometric analysis of the DNA content in control and POL-P3b-treated groups (L: 250, M: 500 and H: 1000 μg/mL) for 72 h.

In this study, we evaluated the anticancer efficacy and associated mechanisms of POL-P3b on cervical cancer in vitro and in vivo. The cytotoxicity of POL-P3b in vitro was detected by MTT assay, and the result indicated that POL-P3b inhibited HeLa cell proliferation at dose- and time-dependent manners (Table 1). The in vivo study demonstrated that 50–200 mg/kg POL-P3b markedly inhibited tumor growth in a dose-dependent manner (Table 2). Thus, we demonstrated

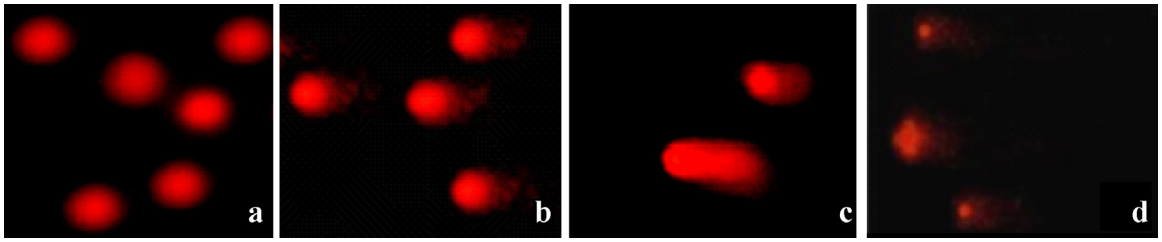

Fig. 4. Effect of POL-P3b on DNA damage. DNA damage was detected using an alkaline comet assay 48 h after POL-P3b treatment in HeLa cells. Photomicrographs of damaged DNA after the various POL-P3b treatments showing an increase in tail moment.

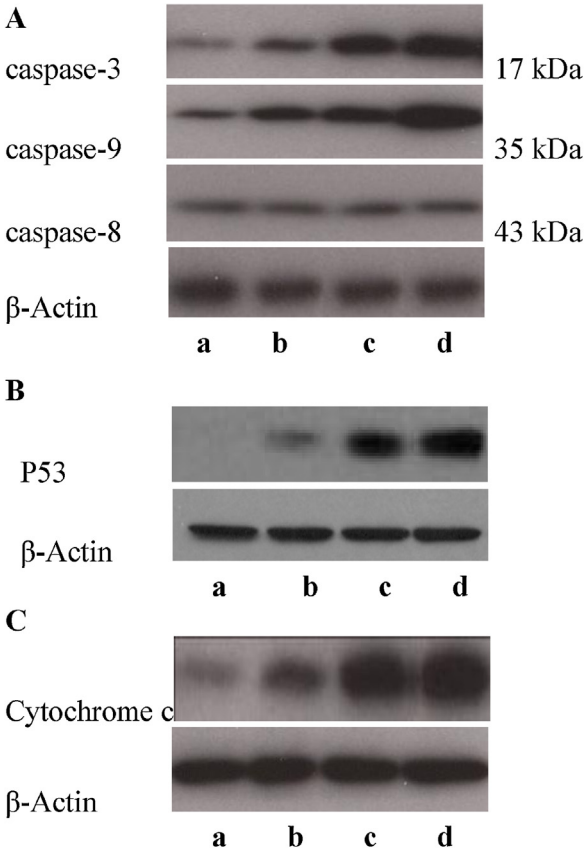

Fig. 5. POL-P3b induced activation of intrinsic/mitochondrial apoptotic pathway. Cells were treated with indicated concentrations of POL-P3b for 72 h, and then the expression levels of p53, caspase-3, 8, caspase-9 and actin protein were analyzed by Western blotting in Section 2 (A and B). β-Actin served as an internal control. Cytosolic cytochrome *c* forms an essential subcomponent of the apoptotic death complex apoptosome, leading to the activation of cellular caspases. To explore the role of mitochondria in the induction of apoptosis by POL-P3b, we examined the mitochondrial release of cytochrome *c* after POL-P3b treatment. Cytochrome *c* was released from the mitochondria into cytosol when HeLa cells were treated with POL-P3b(C).

that POL-P3b inhibited cervical cancer not only in vitro but also in vivo.

Cell cycle progression and apoptosis are two pivotal signaling mechanisms used to maintain homeostasis in healthy tissues. Many anticancer agents arrest the cell cycle at certain phase and then induce cell apoptosis (Kessel and Luo, 2000; Hu et al., 2009; Ashokkumar & Sudhandiran, 2011). In the present study, we found that POL-P3b treatment induced Sub-G1 phase arrest in HeLa cells. This finding will be an additional mechanism of action in retardation of HeLa cell growth by POL-P3b via Sub-G1 phase cell cycle arrest. Indeed, many clinically relevant anticancer agents, such as Lycium barbarum polysaccharides, inhibited cancer cell growth through cell cycle regulation (Zhang et al., 2005). In addition, we demonstrated that POL-P3b treatment not only induced apoptosis in mice xenografted with U14 cells, as evidenced by the increased TUNEL-positive cells, but also showed a significant DNA damage by comet assay.

It is clear that caspase family members play important roles in driving apoptosis (Lavrik, Golks, & Krammer, 2005). Activation of caspase appears to be directly responsible for many of the molecular and structural changes in apoptosis. Among the identified caspases, caspase-3 is thought to be the key enzyme that induces apoptosis. The mitochondria-mediated pathway involves the release of cytochrome *c*, and then followed by the formation of apoptosome, a 140 kDa cytoplasmic complex, consisting of Apaf-1 (apoptotic protease-activation factor-1), dATP, cytochrome *c*, and procaspase-9, which results in activation of caspase-9 and in turn, activating caspase-3 and final fragmentation of DNA. In order to investigate the mechanisms of the POL-P3b-induced apoptosis in HeLa cells, we assessed the release of cytochrome *c* from the mitochondria into the cytoplasm and examined the roles of caspase-3, -8, -9 in POL-P3b-induced HeLa cell apoptosis. Our observation indicated that a significant increase in cytochrome *c* release when HeLa cells were treated with POL-P3b, furthermore, caspase-9 and caspase-3 were activated by POL-P3b in a dose-dependent manner. Tumor suppressor p53 participates in multiple cellular activities including the cell-cycle checkpoints and DNA repair, playing a critical role in maintaining genome integrity and stability (Hartwell & Weinert, 1989). The activation of p53 and related family members can either enforce cell cycle arrest or induce apoptosis. However, more than half of human tumors display p53 mutation or deficiency. We also assessed the expression of p53, and the result showed that cellular level of wild-type p53 protein increased dramatically after POL-P3b treatment. Taken together, it suggested that POL-P3b induced apoptosis involved of the mitochondrial-mediated intrinsic apoptotic pathway. The accumulated p53 triggered apoptosis and led to the release of downstream mitochondrial factors cytochrome *c* from mitochondria to cytosol, and caspase-9 and caspase-3 played key roles in the post-mitochondrial apoptotic pathway. It is possible that POL-P3b induces apoptosis via activation of caspase-9, but not caspase-8 which exists in the vicinity of cell membrane. The activated caspase-9 cleaves the downstream effecter caspases, including caspases-3, which lead to the hallmarks of apoptosis (Boatright & Salvesen, 2003).

5. Conclusions

In conclusion, our results indicated that POL-P3b, the polysaccharide isolated from *P. oleracea* L. as a natural dietary supplement possesses the activity of inhibiting cervical cancer cell growth in vitro and in vivo at a dose- and time-dependent manner, and the mechanisms were associated with cell cycle arrest, triggering DNA damage and inducing apoptosis. It is tempting to speculate that POL-P3b might be utilized as a potential therapeutic agent against cervical cancer. This is only a preliminary study to prove the antitumor effect of POL-P3b on cervical cancer. Further researches about elucidating detailed mechanism of its anticancer actions are in process.

Conflict of interest statement

The authors declare that they have no conflict of interest.

Acknowledgments

We are grateful to sponsor, Science and Technology Project Fund (12511370) of, Department of Education of Heilongjiang Province, PR China.

References

Ashokkumar, P., & Sudhandiran, G. (2011). Luteolin inhibits cell proliferation during Azoxymethane-induced experimental colon carcinogenesis via Wnt/β-catenin pathway. *Investigational New Drugs*, *29*, 273–284.

Boatright, K. M., & Salvesen, G. S. (2003). Mechanisms of caspase activation. *Current Opinion in Cell Biology*, *15*, 725–731.

Chang, S. C., Hsu, B. Y., & Chen, B. H. (2010). Structural characterization of polysaccharides from *Zizyphus jujuba* and evaluation of antioxidant activity. *International Journal of Biological Macromolecules*, *47*, 445–453.

Chen, T., Zhu, L., Liu, X. Y., Li, Y. Y., Zhao, C. D., Xu, Z. G., et al. (2011). Synthesis and antioxidant activity of phosphorylated polysaccharide from *Portulaca oleracea* L.

with H3PW12O40 immobilized on polyamine functionalized polystyrene bead as catalyst. *Journal of Molecular Catalysis A: Chemical*, *342*, 74–82.
Cui, F., Tao, W., Xu, Z., Guo, W., Xu, H., Ao, Z., et al. (2007). Structural analysis of antitumor heteropolysaccharide GFPS1b from the cultured mycelia of *Grifola frondosa* GF9801. *Bioresource Technology*, *98*, 395–401.
Hartwell, L., & Weinert, T. (1989). Checkpoints: Controls that ensure the order of cell cycle events. *Science*, *246*, 629–634.
Hu, Y. W., Liu, C. Y., Du, C. M., Zhang, J., Wu, W. Q., & Gu, Z. L. (2009). Induction of apoptosis in human hepatocarcinoma SMMC-7721 cells in vitro by flavonoids from *Astragalus complanatus*. *Journal of Ethnopharmacology*, *123*, 293–301.
Hung, C. F., Hsu, B. Y., Chang, S. C., & Chen, B. H. (2012). Antiproliferation of melanoma cells by polysaccharide isolated from Zizyphus jujuba. *Nutrition*, *28*, 98–105.
Li, J., Li, Q. W., Peng, Y., Zhao, R., Han, Z. S., & Gao, D. W. (2010). Protective effects of fraction 1a of polysaccharides isolated from *Solanum nigrum* Linne on thymus in tumor-bearing mice. *Journal of Ethnopharmacology*, *129*, 350–356.
Kessel, D., & Luo, Y. (2000). Cells in cryptophycin-induced cell-cycle arrest are susceptible to apoptosis. *Cancer Letters*, *151*, 25–29.
Lavrik, I. N., Golks, A., & Krammer, P. H. (2005). Caspases: Pharmacological manipulation of cell death. *Journal of Clinical Investigation*, *115*, 2665–2672.
Peter, M. E., & Krammer, P. H. (2003). The CD95(APO-1/Fas) DISC and beyond. *Cell Death and Differentiation*, *10*, 26–35.
Schwartsmann, G., Ratain, M. J., Cragg, G. M., Wong, J. E., Saijo, N., & Parkinson, D. R. (2002). Anticancer drug discovery and development throughout the world. *Journal of Clinical Oncology*, *20*, 47S–59S.
Tao, Y. Z., Zhang, Y. Y., & Zhang, L. N. (2009). Chemical modification and antitumor activities of two polysaccharide–protein complexes from *Pleurotus tuberregium*. *International Journal of Biological Macromolecules*, *45*, 109–115.
Wu, H., Guo, H. W., & Zhao, R. (2006). Effect of lycium barbarum polysaccharide on the improvement of antioxidant ability and DNA Damage in NIDDM rats. *Yakugaku Zasshi. Journal of the Pharmaceutical Society of Japan*, *126*, 365–371.
Xiang, L., Xing, D., Wang, W., Wang, R., Ding, Y., & Du, L. (2005). Alkaloids from *Portulaca oleracea* L. *Phytochemistry*, *66*, 2595–2601.
Zhang, M., Chen, H., Huang, J., Zhong, L., Zhu, C. P., & Zhang, S. H. (2005). Effect of *Lycium barbarum* polysaccharide on human hepatoma QGY7703 cells: Inhibition of proliferation and induction of apoptosis. *Life Sciences*, *76*, 2115–2124.
Zhao, L. Y., Dong, Y. H., Chen, G. T., & Hu, Q. H. (2010). Extraction, purification, characterization and antitumor activity of polysaccharides from *Ganoderma lucidum*. *Carbohydrate Polymers*, *80*, 783–789.